Volume 1 | Number 1 | Jan 2013 | Pages 1–100

ROYAL SOCIETY OF CHEMISTRY

ROYAL SOCIETY OF CHEMISTRY

www.rsc.org/materialsB

Robust, self-healing hydrogels from catechol rich polymers

Prabhu S. Yavvari,[1] and Aasheesh Srivastava[1] *

_____

[1]*Department of Chemistry, Indian Institute of Science Education and Research Bhopal, Indore Bypass Road, Bhopal – 462066, Madhya Pradesh, India.*
Fax: (+) 91-755-6692371; Phone: (+) 91-755-6692371
E-mail: asri@iiserb.ac.in

_____

Coordinative interactions between polymer-bound catechols and metal ions are the basis for numerous bio-inspired soft materials. Here, we demonstrate rapid access to catechol rich polymers through reductive amination (RA) strategy. We employed chitosan to exemplify the utility of this protocol. Controlled grafting of catechol pendants (from low-18 mol%, to very high-80 mol%) onto chitosan was readily achieved in aqueous medium under ambient conditions by RA protocol. Due to the high density of catechol units grafted onto chitosan, we could accomplish gelation of water even in acidic medium in presence of transition metal ions, or on addition of chemical oxidant such as $NaIO_4$. Increasing catechol mol% in polymer decreased the amounts of Fe(III) or $NaIO_4$ required to yield gels. UV-vis and Raman studies indicated the presence of mono-complex between Fe(III) and catechol in the gels formed through coordinative crosslinking. Highly ductile hydrogels exhibiting excellent load bearing ability were obtained under these conditions. Electrostatic repulsions between the cationic polymer chains presumably prevented the collapse of gel upon application of load. These gels were also completely self-healing due to the reversible nature of the coordinative interactions. Gels formed at higher pH were brittle and less resilient compared to those formed at lower pH. Ductility and self-healing ability of coordinative cross-linked gels were superior to those formed by oxidative crosslinking. We proffer that RA strategy offers rapid and easy access to catechol-rich systems, and retention of basic amine functionalities allows preparation of robust bio inspired soft materials.

Journal of Materials Chemistry B Accepted Manuscript

1. Introduction

Significant scientific attention is being paid in the recent times to achieve synthesis and processing of soft, non-mineralized load-bearing materials under ambient conditions.[1] Many high-strength biological materials provide inspiring examples of such materials. These include beak and sucker ring of squids,[2-3] and plaques of mussels[4] that employ coordinative and covalent crosslinking of catechol groups of dihydroxyphenylalanine (DOPA) as one of the strategies to achieve their superior performance. The load-bearing ability of catecholic biomaterials is buffeted through coordinative interactions of catechol units with a variety of substrates (stone, metal, wood etc.). Taking cues from such biomaterials, researchers have created a variety of bioinspired polymeric systems containing catecholic functionalities that can be employed as advanced adhesives,[5] stabilizers for nanoparticles,[6] drug delivery systems,[7] and surface coating agents,[8] to name a few. Basic medium (pH ≥8.0) enhances the affinity of catechol units for metal ions, but also accelerates their oxidative oligomerization. Hence, investigations on gels based on catecholic systems have been concentrated around basic pH regime,[5-7] and catechol-assisted gelation in acidic medium is seldom reported.

In synthetic approaches, the catecholic units are invariably appended through amide bond. However, these reactions are usually slow in polymers, and high density of catechol grafting is seldom achieved even after long reaction times. Amide coupling also alters the chemical nature of polyamines by converting the basic amine units into neutral amide functionalities. In this work, we demonstrate ready access to catechol rich chitosan derivatives through reductive amination (RA) protocol. The RA protocol retains the basic nature of amine polymers at all degrees of derivatization. We explored hydrogel formation by these catechol-rich polymers upon coordinative or oxidative crosslinking of catechol pendants. In subsequent sections, we also discuss the mechanical behavior of resulting gels.

2. Results and Discussion

2.1. Preparation and chemical characterization of the polymers

We targeted to achieve high density of catechol grafting on amine polymers while retaining their basic nature. We employed chitosan as a readily-available representative polyamine polymer. Chitosan has been routinely derivatized by amide coupling reaction. However, amide formation alters the chemical architecture of amine polymers, and also requires long reaction times to achieve high degrees of derivatization (DoDs).[11] Hence, we employed the alternative RA strategy for catechol functionalization of chitosan. The RA protocol turned out to be rather straightforward and rapid, and high DoDs were achieved in just a few hours in aqueous medium under ambient conditions without the requirement of any protecting or activating agents (Figure 1a, and Section S1a, ESI for synthetic details). Easy variation of the DoD was achieved – either by varying the equivalents of catechol employed, or by altering the time allowed for the formation of Schiff bases. These results are summarized in Table S1, ESI. The DoDs were found to be 18 mol% (Cat_{C18}), 53 mol% (Cat_{C53}), 66 mol% (Cat_{C66}), and 80 mol% (Cat_{C80}), as calculated from ^{1}H NMR (Figure 1b, and Section S2, ESI for details of calculations). The UV-vis profiles of the catechol grafted polymers showed the presence of a broad band peaking around 280 nm, characteristic of the catechol moieties (Figure 1c).[12] The intensity of this band increased as the DoD increased. All the derivatized chitosans exhibited highly positive zeta potential (ζ) values (Figure 1d). The ζ values of Cat_{C18}, Cat_{C53}, Cat_{C66} and Cat_{C80} polymers were measured to be 35.6, 34.0, 33.1 and 31.7 mV, respectively. These values are rather similar, and are remarkably close to the ζ value exhibited by the unfunctionalized chitosan sample under similar conditions. The large positive ζ values indicate polycationic character of the derivatized polymers. This is the outcome of protonation of the amine repeat units retained in the derivatized chitosans by RA protocol, even at very high degree of catechol grafting.
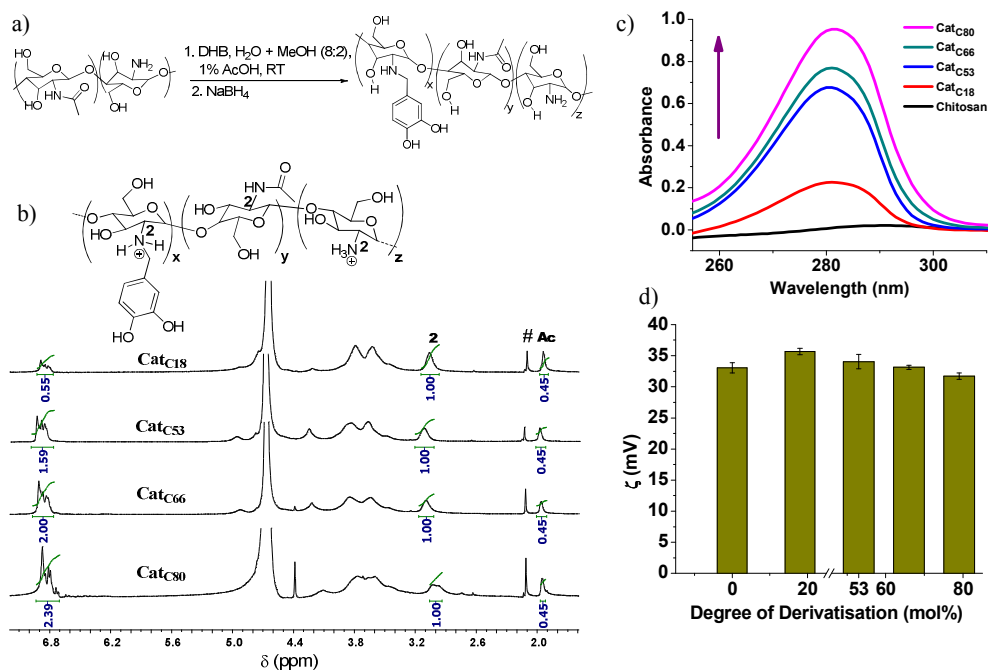
Figure 1. a) Schematic showing the reductive amination (RA) protocol to achieve rapid, high density grafting of catechol units onto chitosan. b) ^{1}H NMR spectra of chitosan derivatized to different extents with catechol units by RA protocol. Peaks marked by # represent the methyl protons of the acetate counter ions to the polymer while those marked by Ac represent the *N*-acetyl groups present in chitosan. The peaks due to the aromatic protons of the catechol units can be observed between 6.7-7.0 ppm. c) UV-vis profiles of the catechol grafted chitosan polymers showing increased intensity of peak around 280 nm with increasing degree of derivatization. d) Zeta potential values for these polymers (measured on three independent samples of each polymer).

2.2. Gel-formation under different stimuli

2.2.1. Gelation through coordinative interactions

An acidic pH (pH ~5) was consciously chosen for further studies since the performance of catechol-based hydrogels in this pH regime is not routinely explored. Acidic medium offers additional advantages that include: (i) minimized aerial oxidation of catechol pendants, (ii) retaining polycationic nature of the polymers due to protonation of amine repeat units, and (iii) minimizing the hydrolysis of certain transition metal (TM) ions such as Fe(III).

Under these conditions, while addition of metal ions such as Ni(II), Zn(II), Nd(II), Eu(III) and Ho(III) to the polymer solutions induced only a mild change in the color and yielded only viscous solutions, addition of Fe(III) and Cu(II) ions induced strong changes in the color of solution, attributed to the coordination of these metal ions to the catechols. We found that these metal ions also induced gelation of aqueous solutions of Cat$_{C66}$ (metal:catechol = 1:2)

even at pH ~3 (ESI, Figure S1 for digital photograph of the gels). A plausible explanation for this rare occurrence of gel-formation with Fe(III) and Cu(II) ions even at low pH values (see the work of Barrett et al.[13] for another example of a dopa containing PEG derivative yielding gels under acidic conditions), and at such low metal concentrations, is the significant higher density of catechol grafted onto these polymers. Previous works utilizing catechol-Fe(III) crosslinks did not achieve gel-formation under acidic conditions either due to lower catechol densities, or because the catechols were part of small molecules.[14] Tethering of multiple catechol units onto each polymer possibly enhances the chelation of Fe(III) ions, and results in gelation even at low pH.

With Fe(III) ions, the gelation process was rather quick and a dark greenish gel was obtained within 10 min. Under the same conditions, Cu(II) ions required overnight incubation to form brownish gels. Thus, the kinetics of gel-formation correlates well with the strength of coordination between the metal ion and catechols ($logK = 20$ and 13.9 for the monocomplex with Fe(III) and Cu(II), respectively).[15] Gels obtained by either Fe(III) or Cu(II) ions were injectable through syringe, and even retained their gelatinous nature immediately upon extrusion from a 19 gauge needle (ESI, Figure S2).

Since the Fe(III) ions were most effective in inducing physical gelation of Cat_{C66} solutions, further investigations into gel-formation employed this metal ion. We noticed that polymers having higher density of catechol grafting, e.g. Cat_{C66}, showed greater propensity to form gels at faster gelation rates when compared to Cat_{C18} and Cat_{C53} having lower density of catechols (ESI, Table S2). The minimum amount of Fe(III) ions required to form gels also decreased as the DoD increased. To illustrate, the minimum Fe(III):catechol could be lowered from 1:3 to 1:22 when going from Cat_{C18} to Cat_{C66}. Further, at constant Fe(III):catechol ratio, the gel-strength (indicated by the G' values of the gels) also increased with increase in the DoD (ESI, Figure S3). The gel formation by the catechol-rich polymers in presence of Fe(III) are summarized as a ternary diagram (Figure 2a).
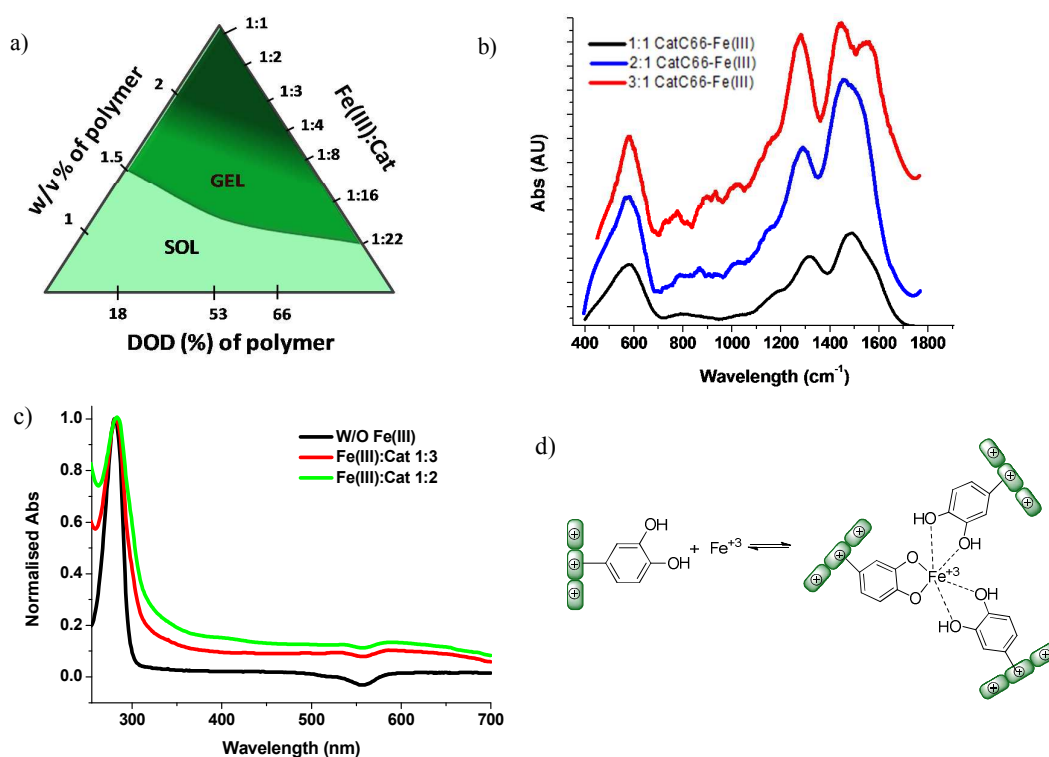
Figure 2. a) Ternary phase diagram indicating the gelation of various catechol derivatised chitosans at different concentrations in presence of varying amounts of Fe(III) ions. Color gradient indicates strength of the resulting gels – darker color implies stronger gels. b) Raman spectra of Cat_{C66}-Fe(III) gels at different Fe(III)-to-catechol ratios. c) UV-vis profiles of Cat_{C66} solutions in presence of varying amounts of Fe(III) ions. d) Schematic showing the formation of monocomplex between catechols and added Fe(III) ion.[14] Based on the experimental evidence, this seems to be the major species present in the hydrogels. The solid lines connecting the catechol to metal indicate coordinative bonds, while the dashed lines indicate electrostatic sorption of catechols.

It is worth mentioning here that at acidic pH, Mentasti *et al*. had reported facile electron exchange between Fe(III) and catechol resulting in production of semiquinone free radicals and Fe(II).[16] The possibility of formation of Fe(II) ions or any semiquinone intermediates was checked by undertaking UV-vis and EPR studies. We did not observe the characteristic peak for the Fe(II)-semiquinone complex in UV-vis at 390-400 nm in our polymer-Fe(III) solutions as was observed by Jameson *et al*.[17] Indeed, in the solid state EPR of the gels formed at Fe(III):catechol of 1:1, 1:2 & 1:3, an explicit signal in the region 1400-1600 G (peak A) characteristic for Fe(III) was observed indicating a Fe(III):catechol complexation (Figure S4, ESI). However, in case of Fe(III):catechol 1:1 and 1:2, a small EPR signal at 3500-3600 G (peak B) was also observed indicating minor formation of Fe(II) in the gels. The

intensity of Fe(II) EPR signal could be correlated with the iron content in the gels. Thus, while peak B in EPR was discernible, even if minutely, at 1:1 coordination ratio (ESI, Figure S4b), it was non-discernible in gels formed at Fe(III):catechol of 1:3 (ESI, figure S4f). However, since the signal intensity is weak and no Fe(II) peak is observable in UV-vis, we believe Fe(III)-catechol complex is still the major, though perhaps not the only, contributor to the gelation process.

We further probed what kind of complex exists between Fe(III) and catechols. We were aware that Szleifer *et al*. have discussed that gels containing ionizable functionalities show significant variation in the pH within the gel compared to that of the bulk.[18] Thus, it is likely that catechols in these hydrogels exist in two populations: a) a major population will be composed of catechols exposed to acidic bulk solvent, and forming monocomplexes with Fe(III) ions, and b) a minor population of catechols may be present within the high pKa niches in the hydrogel, forming complexes of higher coordination number with Fe(III). The gels formed by Cat_{C66} at different coordination ratios (Fe(III):catechol = 1:1, 1:2 or 1:3) showed broad bands in the 470-670 cm^{-1} in the Raman micro spectra (Figure 2b). This band has been attributed to interactions between Fe(III) and oxygen atoms of catechol.[18] However, we must caution that these Raman spectra were recorded in bulk samples and do not exclude a minor population of catechols forming higher coordination complexes with Fe(III). Nevertheless, the UV-vis profiles of Cat_{C66} solution in presence of Fe(III) ions were rather featureless in visible region (Figure 2c), and did not exhibit any peak centered at 500 nm or 550 nm that are attributed to the bis- or the tris- complexes of Fe(III) and catechol, respectively.[19] Hence, based on our current characterization, we can neither confirm nor deny the presence of any minor population of bis and tris Fe-catechol complexes. Based on the literature reports of similar systems,[19c] we conclude that the major species present in these hydrogels is the mono-complex between Fe(III) and catechol (Figure 2d). In such mono-complexes, only one catechol is coordinatively bound to Fe(III) while the other catechol units

undergo electrostatic interaction with this complex due to the supra-molecular cohesive forces. These electrostatically interacting catechols do not form a coordinate bond with the metal center.

2.2.1.1. Viscoelastic properties of the Fe(III)-Cat$_{C66}$ hydrogels

We next initiated investigations into the viscoelastic properties of the gels formed by Cat$_{C66}$ upon addition of Fe(III). We observed that the storage modulus (G′) and the loss modulus (G″) of these gels increased significantly with increase in Fe(III) content in them (Figure 3a). This result is summarized in Figure 3b where the average G′ and G″ values of these gels (mean of moduli in parallel regime of stress-strain profiles) is plotted against the catechol:Fe(III) ratio. As can be seen in Figure 3b, at lower catechol:Fe(III) (i.e. at higher net Fe(III) content in the gel), the G′ value is appreciably higher compared to the G′ value at higher catechol:Fe(III) ratio. This indicates that increasing Fe(III) content in the gels results in greater number of coordinative crosslinks to be formed, and hence the mechanical strength of the gel is increased.
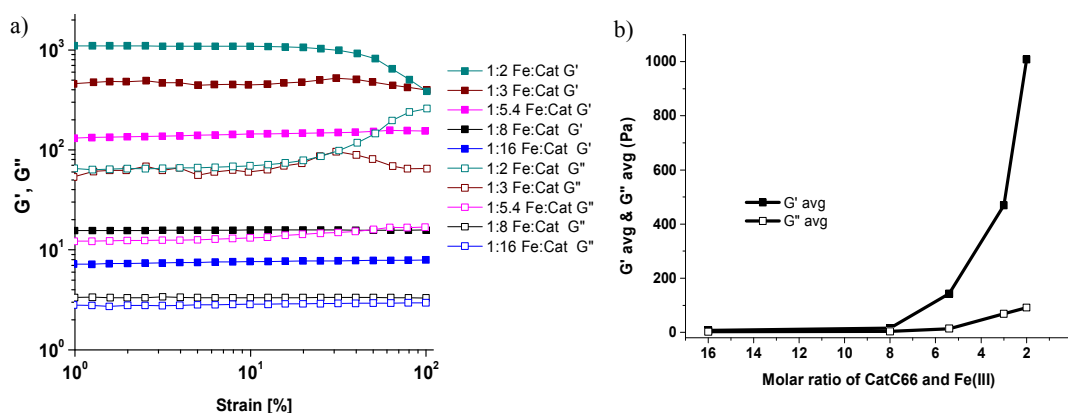
Figure 3. Effect of concentration of Fe(III) on strength of the gels formed by Cat$_{C66}$ at Fe(III):catechol molar ratio of i) 1:2, ii) 1:3, iii) 1:5.4, iv) 1:8, v) 1:16. a) rheological profiles from the amplitude sweep of the gels formed at varying Fe(III):catechol ratios. b) The variation of G′ (filled symbols) and G″ (empty symbols) values (in linear regime of stress-strain curve) for the gels formed by Cat$_{C66}$ at different concentrations of Fe(III). The Fe(III) content in the gels increases from left to right.

The hydrogel formed by Cat_{C66} at Fe(III):catechol of 1:3 (**Fe-Gel**) showed G′ around 800 Pa and retained a parallel regime of both G′ and G″ throughout the range of 1% to 100% strain in amplitude-sweep studies (Figure 3a). Hence, this gel was chosen for further investigations. The **Fe-Gel** was further subjected to a strain-sweep from 1% to 1000% (Figure 4a). The cross-over point (when G″>G′) was reached only beyond 600% strain. This indicates that the **Fe-Gel** resists the oscillatory strain quite effectively. We had also observed that the damping factor (tan δ) remained constant till 40% strain and increased exponentially beyond this point. This indicates that the gel behaves as an elastic solid up to 40% strain, and as a viscoelastic material beyond this strain.

The elastic response of **Fe-Gel** was investigated further using the creep test. In this experiment, we noticed creep ringing phenomenon during initial application of stress (inset of Figure 4b). Creep ringing is generally caused by the coupling of instrument inertia with the elasticity of the viscoelastic sample. The creep ringing behavior observed here is much similar to Jeffrey's model of visco-elastic material supporting the highly elastic behavior of the gel.[20] However, we were more interested in the equilibrium response of these gels rather than their instantaneous response. We found that at longer time scales, **Fe-Gel** also exhibited an immediate elastic response followed by a subsequent delayed elastic response (Figure 4b).
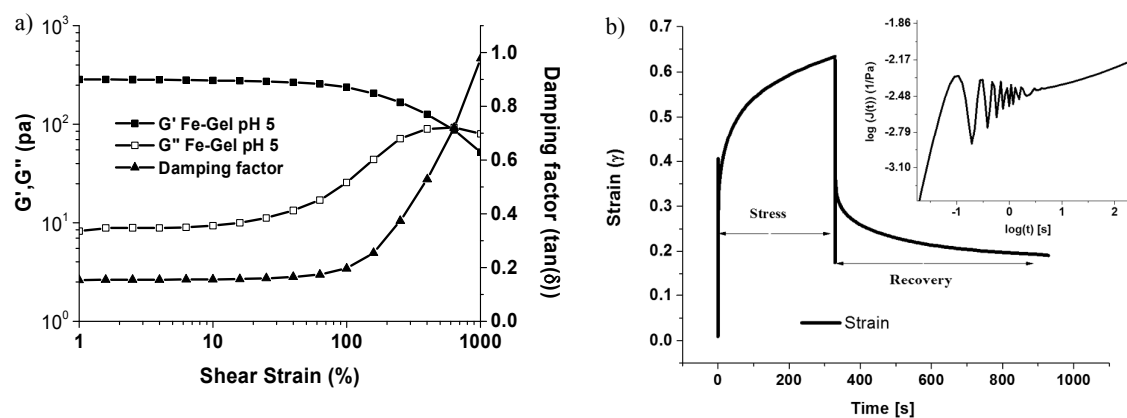
Figure 4. a) Amplitude sweep of the **Fe-Gel** from 1% to 1000% strain and the corresponding modulii and damping factor with respect to the applied strain. b) Creep behavior of the gel under constant shear stress of 100 Pa applied for 330 s followed by recovery. Inset shows the creep compliance (J(t)) vs time (t) during the stress cycle indicating creep ringing observed in the gel in shorter time scale.

We observed that repeated compression and relaxation cycles on **Fe-Gel** produced highly reproducible rheological profiles (ESI, Figure S5). **Fe-Gel** also exhibited an almost linear build-up of stress, as the strain was increased (Figure 5a, filled circles). This linearity was observed up to 1000% applied strain, indicating the highly ductile nature of these gels as well as the ability of these gels to bear high strain without undergoing mechanical disintegration. The amplitude sweep experiments were further analyzed to measure the mechanical energy applied on the gel.[21] In Figure 5b, the G′ and G″ values of **Fe-Gel** are plotted against the mechanical applied energy. This plot shows that an energy of up to 5.1×10^3 J/m^3 needs to be applied to achieve the crossover point.

All of the above indicated that the **Fe-Gels** are resilient enough to bear applied loads without undergoing degradation. A visual demonstration of the gel's ability to bear large amounts of weight is provided in Figure 5c. The gel made from only 32 mg of Cat_{C66} could bear up to 263 g of weight without undergoing mechanical disintegration. The gel showed barrelling on applying weight due to the compressive force of the load, but no permanent distortion in the gel was observed. The gel regained its original dimensions immediately on removal of the load (as shown in panel (iii) of Figure 5c and the embedded video in ESI). Finally UTM analysis was undertaken for **Fe-Gel** that indicated that the gel was able to take a compressive load of 4.4 N while undergoing a compressive extension up to ~70% of its initial height (10 mm) before undergoing disintegration (ESI, Figure S6). The load bearing capability and the shape-retention on removal of load is ascribed to the combined influence of the electrostatic repulsions between the polycationic polymer chains and the reversible coordinative interactions holding the gels together. Together, these interactions impart ductility to the gels by preventing the collapse of polymer chains even under very high stress,[22] and also help the gel to revert to its original shape after removal of the load. These results highlight that the sacrificial and reversible nature of coordinative interactions can be utilized to create materials with good load bearing abilities due to the preferential breaking and ready reforming of these

crosslinks during the loading and unloading stages, respectively.[23] Lee *et al.* have also

reported augmentation of the strength of spider silk fibers by infiltration with metal ions.[24]
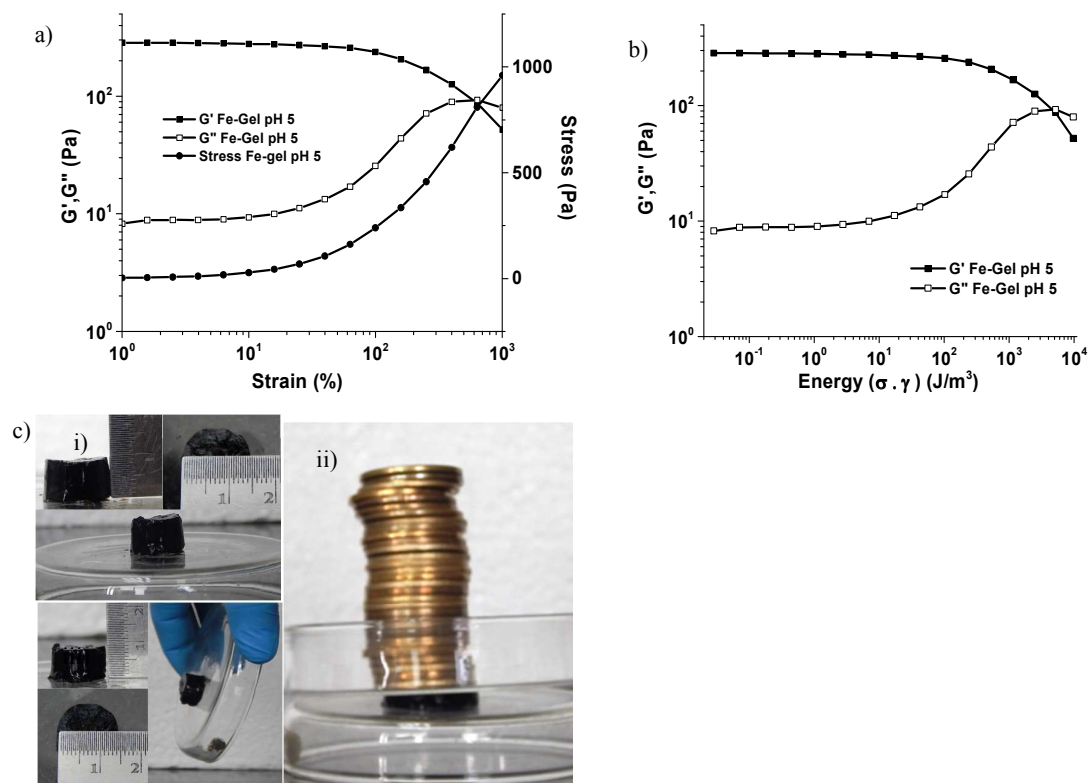
Figure 5. Mechanical studies on **Fe-Gel** prepared at pH 5. a) Changes in the storage modulus (G′) and loss modulus (G″) and stress profiles obtained from the amplitude-sweep rheology experiment (strain 1% - 1000%). b) Dynamic storage and loss modulii of the gels plotted versus applied energy during the amplitude sweep rheology experiment.[21] c) Visual demonstration of load bearing ability of gels prepared at pH 5. i) Initial dimensions of the gel before applying load; ii) gel bearing the applied load; iii) immediate recovery of gel to original dimensions, upon removal of load. Refer to text for details. Video provided in ESI.
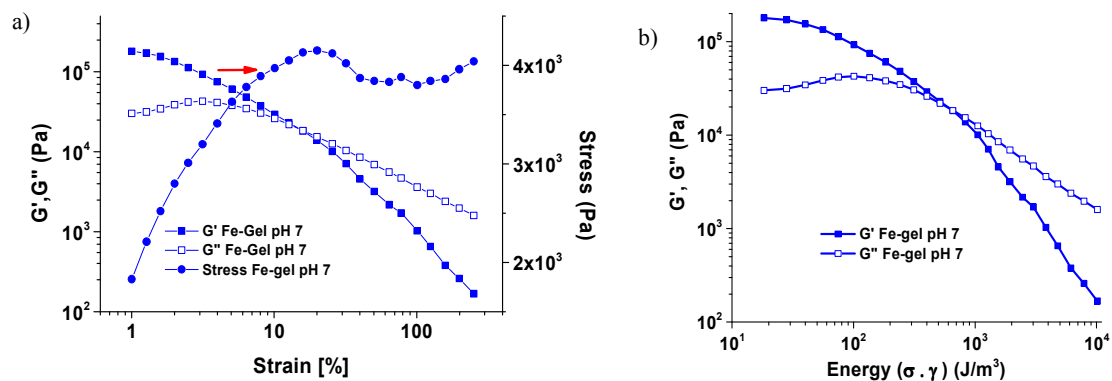
Figure 6. Rheological investigations on **Fe-Gel** equilibrated at pH 7. a) Storage modulus (G′), loss modulus (G″) and stress profiles (red arrow indicate yield point) obtained from the amplitude sweep experiment. b) Dynamic storage and loss modulii of the gels plotted versus applied energy (σ.γ (J/m^3)) during the amplitude sweep.[21].

Table 1. Summary of mechanical properties of the gels.

Hydrogel	Critical stress (σ_c, Pa)	Critical strain (γ_c)	Critical Shear modulus (σ_c/γ_c) (Pa)	Energy[a] applied up to cross-over point (J/m³)
Fe-Gel (pH 5)	800	6.40	125	5.14×10^3
Fe-Gel (pH 7)	4100	0.15	27300	0.615×10^3
Ox-Gel[b] (pH 5)	260	0.31	830	0.078×10^3

[a]Energy applied per unit volume = Shear stress(σ)·Shear strain(γ)).[21] [b]**Ox-Gel** are the gels formed by the oxidative crosslinking of Cat_{C66} with $NaIO_4$ (1:17 $NaIO_4$:catechol), see section 2.2.2.

In order to test the hypothesis of the role of polycationic backbone on mechanical properties of the gel, the **Fe-Gel** was equilibriated in a neutral phosphate buffer (pH 7.0). The resultant buffered gels showed profound increase of the G′ and G″ values (1.8×10^5 and 3.0×10^4 Pa, respectively) in amplitude-sweep experiments (Figure 6a). Also, while **Fe-Gel** at pH 5 showed almost linear elastic response up to 1000% strain (Figure 5a), the buffered gels exhibited a linear elastic response only up to 8% strain (yield point indicated by red arrow in Figure 6a). As a result of enhanced brittleness, these gels could resist an applied energy of only up to 0.615×10^3 J/m³ (Figure 6b), merely one tenth the energy taken by **Fe-Gel** at pH 5. These results are summarized in Table 1. This can be attributed to a combined influence of stronger metal complexation, decreased electrostatic repulsions between the polymer backbone in gel network, and probable formation of additional crosslinks due to some oxidative crosslinking. The enhanced strength of these gels, however, was offset by the brittleness of the gels with the crossover point at only 14% strain in the buffered gels.

2.2.2. Gelation by oxidative crosslinking

Catechol based systems are also known to undergo oxidative crosslinking in presence of $NaIO_4$ due to the oxidization of catechol to 1,2-benzoquinone that is capable of self-crosslinking (Figure 7a), as well as reacting with nucleophiles such as amines or thiols. We explored gel-formation under oxidative conditions by our catechol-grafted chitosan polymers. All the polymers yielded gels upon addition of periodate (ESI, Figure S7a for digital

photographs of gels). The gels obtained by oxidative crosslinking were also injectable (ESI, Figure S7b). For Cat_{C18} and Cat_{C53}, gels were formed at periodate:catechol molar ratio of 1:2.6 and 1:53, respectively, while Cat_{C66} formed gel even at ratio of 1:100 (periodate:catechol). Thus, polymers having higher density of catechol-grafting required smaller amounts of periodate to form gels. UV-vis profiles of the Cat_{C66} polymer solution in presence of $NaIO_4$ indicated the oxidation of catechol to form quinones (Figure 7b). However, the acidic pH would significantly decrease the nucleophilicity of the functionalized glucosamine units, thus encouraging the preferential oligomerization of the catechol moieties.[25]
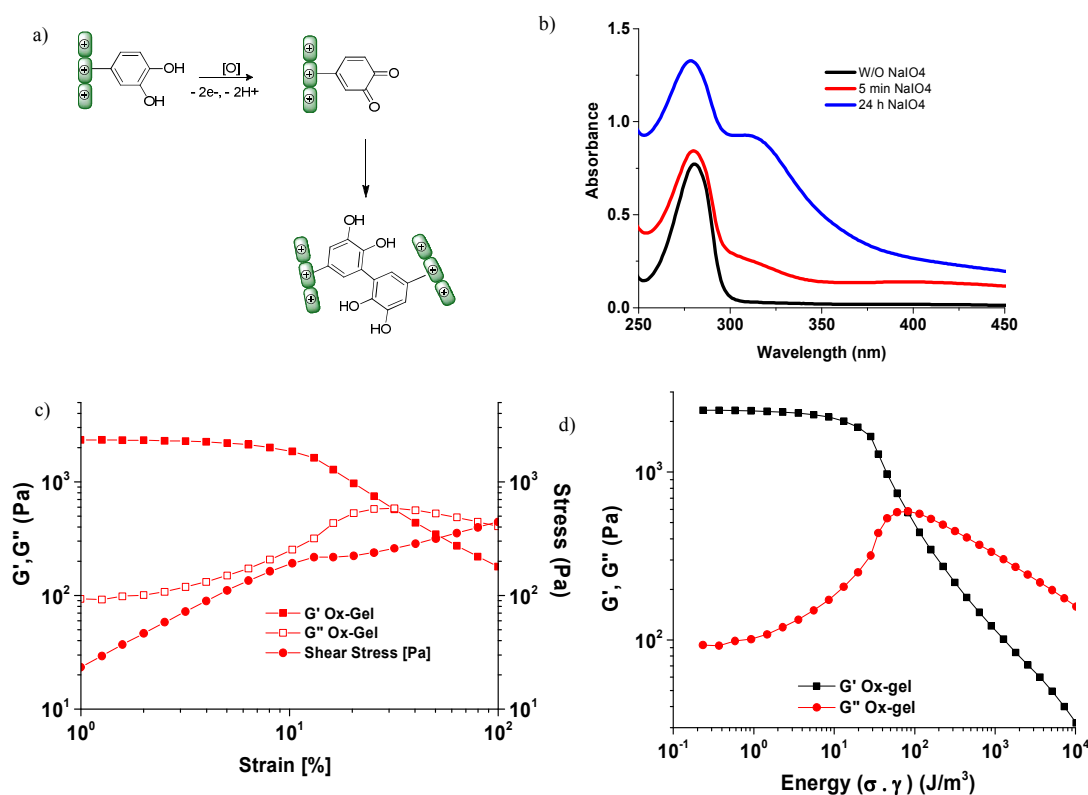
Figure 7. a) Schematic showing oxidative dimerization of the catechol moieties upon addition of $NaIO_4$. This results in covalent cross linking of catechol derivatised polymers. b) Time-dependent evolution of UV-vis profile of Cat_{C66} solution over the course of 24 h after addition of $NaIO_4$. c) Changes in dynamic storage and loss modulii as well as changes in shear stress versus strain, for **Ox-Gel** (formed at 1:17 $NaIO_4$:catechol by Cat_{C66}). d) Dynamic storage and loss modulii of the **Ox-Gel** plotted versus applied energy ($\sigma.\gamma$ (J/m^3)) during the amplitude sweep.[20]

The gels formed by Cat_{C66} at $NaIO_4$:catechol = 1:17 (**Ox-Gel**) were employed for rheological studies. While **Ox-Gel** had higher G′ values compared to the **Fe-Gel** (G′ value at initial strain = 2373 Pa and 278 Pa, respectively), they showed a clear crossover near 13% strain (Figure 7c). The linear elastic response of the **Ox-Gels** was observed only up to 13% strain, almost an order of magnitude lesser than that observed for the **Fe-Gel** (Figure 4a). As can be seen in Table 1 and Figure 7c, the **Ox-Gel** had a lower critical stress of 257 Pa which is almost one third to that of **Fe-Gel** and also could take an energy up to 0.078×10^3 J/m^3 before undergoing crossover (Figure 7d). Thus, the **Ox-Gel** exhibited greater brittleness and lower energy absorbing ability when compared to **Fe-Gel**.

To summarize, we observed that gels formed by coordinative crosslinking at pH 5 were able to absorb much more energy than the same gels buffered at pH 7; while the gels formed under oxidative conditions through covalent crosslinking were able to absorb the least amount of energy. This is graphically depicted in Figure 8.
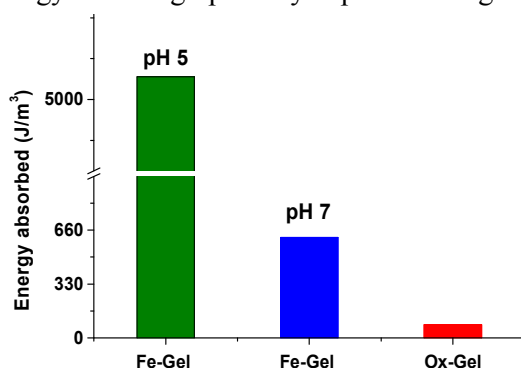
Figure 8. Relative amount of energy absorbed before reaching the cross-over point for gels prepared under different conditions (**Fe-Gels** at pH 5 and 7, and **Ox-Gel** at pH 5).

2.3. Self-healing ability

Gels having a dynamic equilibrium between their component functional groups are known to demonstrate self healing behavior. In the gels reported in this work, coordinative crosslinks are highly dynamic and can be broken and reformed readily. Further, when stress is applied to these gels, electrostatic repulsions between cationic polymer backbone probably cause the polymer chains to slide upon, rather than collapse onto, each other. However the extent of

such sliding cannot be infinite, and hence, beyond certain strain and stress values the gels would yield. The recovery of these gels would depend upon ready re-formation of the crosslinks once the stress is removed. Researchers have realized that the coordinative interactions between catechols and Fe(III) ions are highly reversible and act as sacrificial bonds that rupture under high stress, but readily reform on removal of stress.[11,25,26] This dynamic equilibrium helps to rapidly stabilise the gel network under stress and allows for quick reformation of the gels. We tested the self-healing ability of the gels prepared at pH 5 (both **Fe-Gels** and **Ox-Gels**) by two separate methods. The gels were subjected to a degradation by amplitude sweep (linear time sweep) from 1% to 1000% strain and then allowed to heal under 0% strain for 100 s. In this experiment, strain applied to the gels is increased gradually. In a separate experiment, the gels were also subjected to degradation by applying a high sudden strain at 1000% (a non-linear time sweep) and their healing ability was investigated. Under these conditions, there is a sudden input of energy, and the gel network may not get sufficient time to re-organize itself in response to applied strain. Hence, the non-linear time sweep can result in greater degradation of the gels. As can be seen in Figures 9a and 9b, the **Fe-Gels** showed rapid healing and complete regaining of its pristine strength within a short time span of 100 s in both the cases, *viz.* under linear as well as non-linear time sweep. A rough visual demonstration of the healing ability of **Fe-Gel** is provided in the video embedded in ESI. The self-healing ability was also observed even when the **Fe-Gels** were exposed to neutral phosphate buffer (pH ~7.0, Figure 9c and 9d). The gel regained its original strength after the healing cycle, probably due to the sacrificial and reversible nature of Fe(III)-catechol bonds. The **Fe-Gels** (at pH 5.0 and pH 7.0) also showed a slight increase in the G′ values under high strain (1000%) (Figure 9b & 9d) which further indicates rapid reversible crosslinking occurring within the gels. When **Ox-Gels** were subjected to linear time sweeps, they too showed significant healing in terms of regaining their initial G′ and G″ values after each cycle (Figure 9e). However, upon sudden application of high strain

in the non-linear time sweep experiment, though **Ox-Gels** too showed slight increase of G′ values under high strain (1000%), there was a continuous drop in G′ values after each cycle for these gels (Figure 9f). This indicates that the **Ox-gels** have a limited ability to heal only when the polymer chains get enough time to respond to the applied strain, and not otherwise. Under high sudden strain, the irreversible nature of covalent crosslinks in the **Ox-Gels** results in incomplete healing. Contrastingly, the dynamic nature of coordinative interactions allow for quick re-healing of the **Fe-Gel**, irrespective of the rate at which strain is applied.
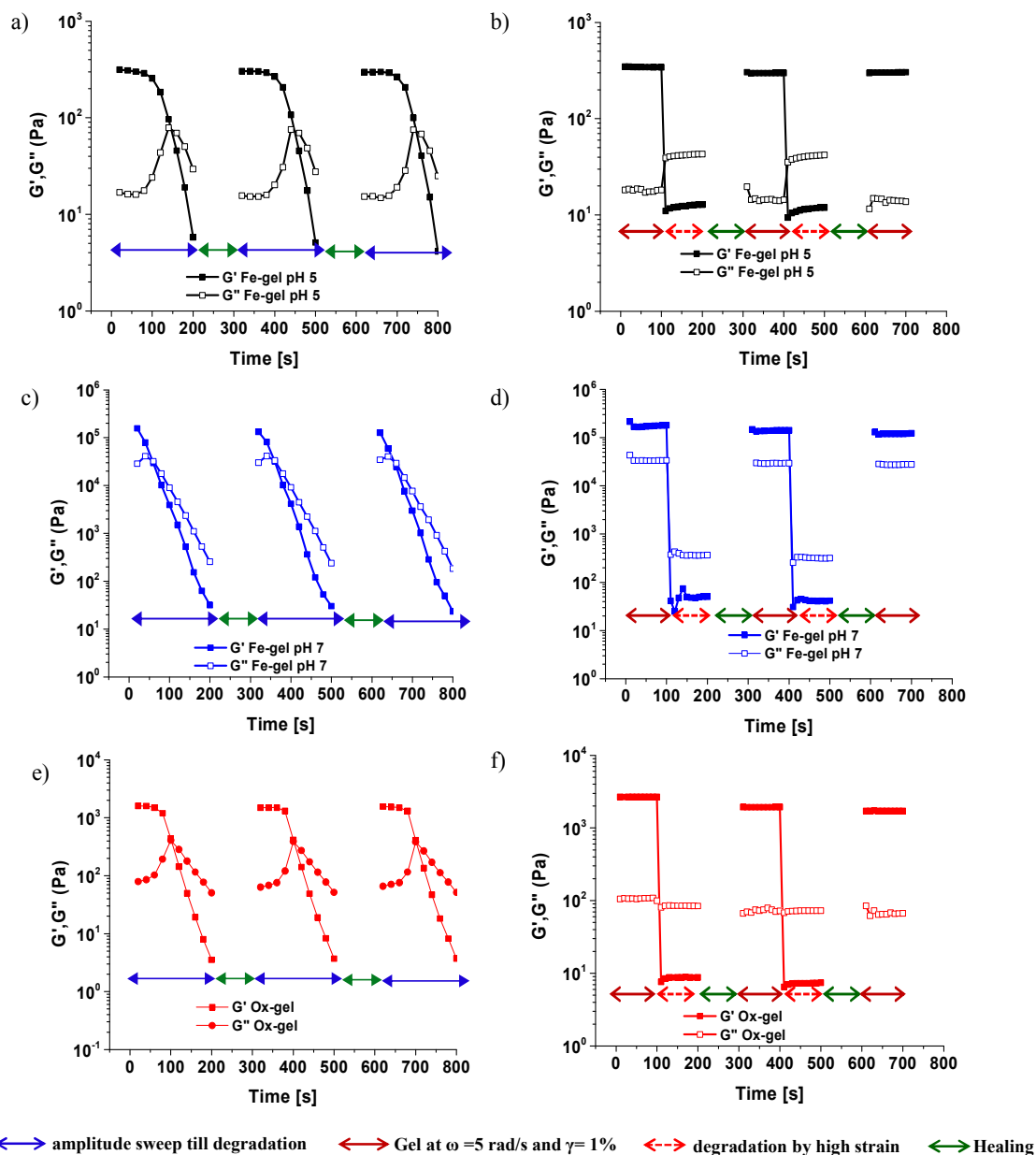
Figure 9. Rheological demonstration of self-healing ability of the hydrogels. Rheological profiles on left panels (a, c and e) are for linear time sweep experiments while those on right (b, d and f) are for non-linear time sweep experiments (see experimental section for details). Top panel (a, b) is for **Fe-Gel** at pH 5; middle panel (c, d) is for **Fe-Gel** equilibrated at pH 7 while the bottom panel (e, f) is for **Ox-Gel.** The degradation and healing is shown for two cycles.

3. Conclusions

In conclusion, we have demonstrated the utility of reductive amination (RA) to achieve facile and controlled attachment of catechols (as a DOPA surrogates) on to amine polymers, chitosan being the representative polymer in this study. Due to the high density of catechol grafting achievable by RA strategy, these chitosan derivatives could form gels even in acidic

medium upon addition of Fe(III) and Cu(II) ions as coordinative crosslinkers, or in the presence of $NaIO_4$ as oxidant. Under these conditions, the mono-complex between Fe(III) and catechols was found to be the major species present in the gels. Minor existence of semiquinone species was also observable at high Fe(III) loadings in the gels. The protonation of amines retained in these polymers resulted in electrostatic repulsions between polycationic polymer chains, countering the coordinative interactions between catechols and Fe(III). Consequently, these gels were highly ductile, injectable, and had good load bearing abilities. Complete retention of shape on removal of the applied load was observed for these gels. Gels buffered in neutral phosphate buffer had higher stiffness but were also more brittle. The gels formed by oxidative oligomerization of catechols using periodate had the most inferior mechanical performance. In their self-healing ability also, gels formed by coordinative crosslinking were more effective than those formed by the oxidative crosslinking. We have thus shown a simple and rapid protocol to obtain catechol rich polymers that yield hydrogels with unique mechanical properties.

4. Experimental Section

4.1. Materials and Methods

All chemicals employed in this work were from commercial sources, and were used without further purification. Dialysis tubings (MWCO ~10 kDa) were obtained from Sigma. All the studies were performed using stock solutions of 2% w/v polymer in 1% aqueous acetic acid, unless stated otherwise. ^{1}H NMR spectra were recorded in D_2O at 8 mg/mL polymer concentrations on a Bruker Ultra shield (400 MHz) spectrometer. UV-vis absorption spectra were recorded on PerkinElmer Lambda25 spectrophotometer. Zeta potential values of the polymers were measured on Beckman Coulter Delsa Nano C instrument using flow cell. Raman microspectra of gel samples were recorded on LabRam HR Horiba scientific instrument. All the rheological experiments were performed using Rheoplus MCR102

(Anton-Paar) rheometer using a 25 mm cone plate geometry with cone angle being 1° at measuring distance of 0.05 mm at temperature of 25 °C. A wet sponge is placed around the cone plate and base plate of the rheometer to act as a solvent trap.

4.2 Polymer synthesis and chemical characterizations

Detailed synthetic protocols are provided in the ESI, section S1. The DoDs of catechol functionalities in the resulting polymers were inferred from ^{1}H NMR spectra (see ESI, section S2). Chitosan polymers with 18, 53, 66 and 80 mol% grafting were obtained. These polymers were named as Cat_{C18}, Cat_{C53}, Cat_{C66} and Cat_{C80}, respectively.

4.3 UV-vis and Zeta potential studies

For UV-vis study on grafted polymers, the polymer stock solutions were diluted to 0.001% w/v and filtered using 0.45 µm syringe filters.

To investigate the interaction of Cat_{C66} polymer with either Fe(III) or $NaIO_4$ by UV-vis, the following protocol was adopted. A stock solution of 0.006% w/v Cat_{C66} was prepared by diluting the 2% w/v of Cat_{C66} polymer solution. To 1 mL of this solution, requisite volume of 0.006 M $Fe(NO_3)_3$ solution was added to obtain the Fe(III):catechol of 1:3 and 1:2, respectively, before recording the UV-vis spectra. The resultant spectra were normalized with respect to absorption maxima at 281 nm. Similarly, 0.006 M $NaIO_4$ was added to get $NaIO_4$:catechol = 1:17 and the spectra of the solution were recorded after 5 min and after 24 h to check the oxidation of catechols.

For the zeta potential measurements, the polymer stock solutions diluted to 0.02% w/v were used. The underivatised chitosan was used as a control at a same concentration. The measurements for each sample were triplicated and the average of the values was reported.

4.4 Preparation of hydrogels

4.4.1 Gelation by coordinative crosslinking

Cat_{C66} – the polymer containing maximum catechol units and giving fluid solutions at 2% w/v concentration in aqueous acidic medium – was chosen for this investigation. To 500 µL samples of Cat_{C66} at 2% w/v concentration in individual vials, were added 100 µL of 0.2 M solutions of different metal salts. These mixtures were vortexed for 10 s to ensure uniform mixing and left undisturbed for 12 h. Gelation was inferred from the ability of the sample to support its weight upon inversion of the vial. For Cu(II) and Fe(III), the gelation kinetics were investigated further by tilting the samples at different time-points, and observing the resistance to flow. To probe the effect of DoD on the gelation kinetics, calculated volumes of 0.2 M $Fe(NO_3)_3$ were added to 500 µL of 2% w/v solutions of each polymer to reach final Fe(III):catechol ratio of 1:2. The minimum Fe(III) concentration required for gelation was measured by adding 100 µL of 0.1 M, 0.08 M, 0.06 M, 0.04 M, 0.02 M or 0.01 M solutions of $Fe(NO_3)_3$ to 500 µL of Cat_{C66} polymer solutions (2% w/v) in different glass vials. The gels formed at Fe(III):Cat_{C66} -1:3 (**Fe-Gels**) showed a pH around 5 whereas, those gels formed at higher concentrations of Fe(III) showed a pH around 3 to 4. The resulting mixtures were vortex shaken for 10 s and monitored for next 24 h for gel-formation.

4.4.2 Gelation by oxidation

To 500 µL of individual polymer solution (2% w/v) in 5 mL glass vials, 10 µL of 0.18 M $NaIO_4$ solution was added while vortexing, and the mixture monitored for gelation. Under these conditions, a reddish-brown gel formed after 5 min in case of Cat_{C66}, after 30 min for Cat_{C53} and after 9 h for Cat_{C18}. (Gels formed with $NaIO_4$: catechol greater than 1:17 induced a pH lower than 5). For rheological characterization, gels were formed by mixing 20 µL of 0.18 M $NaIO_4$ to 800 µL of 2% w/v polymer ($NaIO_4$: catechol = 1:17, **Ox-Gels**). The resulting mixtures were immediately transferred into cylindrical casts and allowed to set for 6 h at 23

°C. The gels thus formed were subjected to amplitude sweep from 1% to 1000% strain at angular frequency of 5 rad/s.

4.5 Raman Spectroscopy of Fe-Gels

The solutions of Cat_{C66} polymer and $Fe(NO_3)_3$ prepared at varying coordination ratios of Fe(III):catechol = 1:1, 1:2 and 1:3) were cast into thin films on glass layer, and dried in oven at 40 $^{\circ}$C for 6 h. Raman spectra of the above prepared samples were recorded with diode-pumped laser excitation wavelength of 632.8 nm and D 0.3 filter using 50x eyepiece. The spectra were acquired using an air-cooled CCD. Since the samples were sensitive to burning by the laser beam, each collected spectra consisted of 100 accumulations of a 0.2 s integration time. For each sample, three spectra collected from different regions of the sample were averaged and smoothed with a Savitzky-Golay smoothing filter and normalised with respect to the maximum absorbance at 1500 cm^{-1}.

4.6 EPR spectrocopy of the Fe-Gels.

The solutions of Cat_{C66} and $Fe(NO_3)_3$ prepared at different coordination ratios (Fe(III):catechol = 1:1, 1:2 and 1:3) were allowed to set for 6 h in closed vials and were lyophilized subsequently. The resulting dried samples were analyzed using EPR performed on Bruker micro X. (Parameters used: X band, operating frequency 9.450301 GHz, Receiver gain - 1.26× 10^3, Modulation frequency – 100 kHz, Modulation amplitude – 21.04 G).

4.7 Mechanical characterizations of the Fe(III)-crosslinked gels

4.7.1 Influence of DoD on mechanical strength of gels

To investigate the influence of DoD on the mechanical strength of the resulting hydrogels, the samples were prepared at constant Fe(III):catechol = 1:2 for all the polymers. For this, variable volumes of 0.2 M Fe (NO_3)$_3$ were added to 800 µL of 2% w/v solutions of individual polymers (Cat_{C18}, Cat_{C53} or Cat_{C66}). The resulting solutions were then transferred into covered cylindrical casts and were allowed to set for 6 h at 23 °C, before undertaking the rheological

studies where the gels were subjected to amplitude sweep of 1% to 100% strain at a constant frequency of 5 rad/s.

4.7.2 Influence of coordination ratio on the gel-strength

To investigate the influence of varying the Fe(III):catechol on the strength of gels, samples were prepared by mixing 800 μL of 2% w/v of Cat_{C66} solution with 200 μL of $Fe(NO_3)_3$ solutions of various concentrations (*viz*. 0.2 M, 0.1 M, 0.08 M, 0.06 M, 0.04 M, 0.02 M). The resulting solutions were then transferred into covered cylindrical casts and were allowed to set for 6 h at 23 °C. The resulting gels were then subjected to amplitude sweep of 1% to 100% strain at a constant frequency of 5 rad/s.

Creep studies were performed on the gels formed at Fe(III):catechol = 1:3 at pH = 5, since these gels had the most optimal strength and elasticity. In the creep tests, a shear stress of 100 Pa was applied and held constant while measuring the resulting shear strain of the gels as a function of time.

Influence of pH on gel behavior: The gels were prepared by mixing 2% w/v Cat_{C66} polymer solution in 1% Acetic acid and 0.1 M $Fe(NO_3)_3$ at Fe(III):catechol = 1:3 and pH = 5. The mixture was mixed well and was transferred into cylindrical cast without any further delay (through which gels of 1.0 cm inner diameter and 0.5 mm height were formed). The resulting gels were allowed to set for 6 h at 23 °C and then they were further treated with 0.1 M phosphate buffer at pH = 7.0 for 2 h. Later the gels were subjected to amplitude sweep of 1% to 1000% strain at constant frequency of 5 rad/s.

4.7.3 Load-bearing and self-healing properties

To visually demonstrate the load bearing ability of these gels, a representative gel was prepared by mixing 2% w/v Cat_{C66} polymer solution in 1% Acetic acid and 0.1 M $Fe(NO_3)_3$ at Fe(III):catechol = 1:3 and of pH 5. The mixture was mixed well and with no delay is transferred into covered cylindrical cast (through which gels of 1.5 cm inner diameter and 1 cm height were prepared). After the gel was allowed to set for 6 h, the gel was carefully

extruded out of the cast. A pre-weighed petri dish (40 g) was placed on the gel and onto it, coins (approx. 7 g each) were placed in increasing numbers.

For rheological demonstration of self-healing ability of the **Fe-Gel**, the gel prepared by mixing 2% w/v Cat_{C66} polymer solution in 1% Acetic acid and 0.1 M $Fe(NO_3)_3$ at Fe(III):catechol = 1:3 and of pH 5 was immediately transferred into cylindrical casts and allowed to set for 6 h. For the effect of pH on **Fe-Gel**, the gel formed at similar composition was treated with 0.1 M phosphate buffer of pH~7.0 further for 2 h. Similarly, the **Ox-Gels** were prepared by mixing 20 μL of 0.18 M $NaIO_4$ to 800 μL of 2% w/v polymer ($NaIO_4$: catechol = 1:17). The resulting mixtures were immediately transferred into cylindrical casts and allowed to set for 6 h. The gels thus prepared were subjected to two types of degradation. In the linear time sweep study, the gel was subjected to degradation by applying an amplitude sweep of 1% to 1000% strain at an angular frequency of 5 rad/s for 200s and then the gel is allowed to heal for 100s at 0% strain. The gel was then further subjected to amplitude sweep for degradation and subsequent healing for one more cycle. In the a non-linear time sweep experiment, where the initial G′ and G″ gel was recorded at 1% strain and angular frequency of 5 rad/s for 100 s, and then a sudden strain of 1000% (angular frequency of 5 rad/s) was applied for 100 s to degrade the gel. The sample was allowed to heal for 100 s at 0% strain before subjecting it further to one more cycle of degradation followed by healing.

4.7.4. UTM analysis:

UTM was done on Instron Universal testing machine Model 3382 (100 N-100 kN). The gel was prepared by mixing 2% w/v Cat_{C66} polymer solution in 1% Acetic acid and 0.1 M $Fe(NO_3)_3$ at Fe(III):catechol = 1:3 and pH = 5. The mixture was mixed well and with no delay is transferred into cylindrical cast (through which gels of 1.5 cm inner diameter and 1 cm height were prepared). The gel was cured for 6 h before undertaking UTM analysis. The compressive load was applied at an approach rate of 1.3 mm/min.

Supporting Information

Supporting Information is available [Includes synthesis of polymer, rheological profiles of the hydrogels formed by coordinative crosslinking and those formed by covalent cross linking, videos of load-bearing and self-healing of the gel].

Abbreviations DOPA -Dihydroxyphenylalanine, DHB -Dihydroxybenzaldehyde, RA-Reductive amination, DoD- Degree of Derivatization, UTM- Universal testing machine

REFERENCES

[1] a) P. Sahoo, R. Sankolli, H.-Y. Lee, S. R. Raghavan, P. Dastidar, *Chem. Eur. J.* **2012**, *18*, 8057–8063; b) Q. Chen, L. Zhu, C. Zhao, Q. Wang, J. Zheng, *Adv. Mat.* **2013**, *25*, 4171–4176; c) H. Bodugoz-Senturk, C. E. Macias, J. H. Kung, O. K. Muratoglu, *Biomaterials* **2009**, *30*, 589–596; d) C. W. Peak, J. J. Wilker, G. Schmidt, *Colloid Polym. Sci.* **2013**, *291*, 2031–2047; e) L. Hsu, C. Weder, S. J. Rowan, *J. Mater. Chem.* **2011**, *21*, 2812–2822.

[2] A. Miserez, T. Schneberk, C. Sun, F. W. Zok, J. H. Waite, *Science* **2008**, *319*, 1816–1819.

[3] a) A. Miserez, J. C. Weaver, P. B. Pedersen, T. Schneeberk, R. T. Hanlon, D. Kisailus, H. Birkedal, *Adv. Mater.* **2009**, *21*, 401–406; b) A. Miserez, D. Rubin, J. H. Waite, *J. Biol. Chem.* **2010**, *285*, 38115–38124.

[4] J. H. Waite, M. L. Tanzer, *Science* **1981**, *212*, 1038–1040.

[5] a) D. G. Barrett, G. G. Bushnell, P. B. Messersmith, *Adv. Healthcare Mater.* **2013**, *2*, 745–755; b) C. R. Matos-Pérez, J. D. White, J. J. Wilker, *J. Am. Chem. Soc.* **2012**, *134*, 9498–9505; c) C. R. Matos-Pérez, J. J. Wilker, *Macromolecules* **2012**, *45*, 6634–6639; d) L. Ninan,

R. L. Stroshine, J. J. Wilker, R. Shi, *Acta Biomaterialia* **2007**, *3*, 687–694; e) L. K. Mann, R. Papanna, K. J. Moise Jr., R. H. Byrd, E. J. Popek, S. Kaur, S. C. G. Tseng, R. J. Stewart, *Acta Biomaterialia* **2012**, *8*, 2160–2165; f) S. Kaur, G. M. Weerasekare, R. J. Stewart, *ACS Appl. Mater. Interfaces* **2011**, *3*, 941–944; g) S. H. Yang, S. M. Kang, K.-B. Lee, T. D. Chung, H. Lee, I. S. Choi, *J. Am. Chem. Soc.* **2011**, *133*, 2795–2797; h) C. E. Brubaker, P. B. Messersmith, *Biomacromolecules* **2011**, *12*, 4326–4334; i) J. H. Ryu, Y. Lee, W. H. Kong, T. G. Kim, T. G. Park, H. Lee, *Biomacromolecules* **2011**, *12*, 2653–2659; j) S. Hong, K. Y. Kim, H. J. Wook, S. Y. Park, K. D. Lee, D. Y. Lee, H. Lee, *Nanomedicine* **2011**, *6*, 793–801; k) I. You, S. M. Kang, Y. Byun, H. Lee, *Bioconjugate Chem.* **2011**, *22*, 1264–1269.

[6] a) Y. Lee, H. Lee, P. B. Messersmith, T. G. Park, *Macromol. Rapid Commun.* **2010**, *31*, 2109–2114; b) K. C. L. Black, Z. Liu, P. B. Messersmith, *Chem. Mater.* **2011**, *23*, 1130–1135; c) S. M. Kang, N. S. Hwang, J. Yeom, S. Y. Park, P. B. Messersmith, I. S. Choi, R. Langer, D. G. Anderson, H. Lee, *Adv. Funct. Mater.* **2012**, *22*, 2949–2955;

[7] J. Su, F. Chen, V. L. Cryns, P. B. Messersmith, *J. Am. Chem. Soc.* **2011**, *133*, 11850–11853.

[8] a) S. Ryu, Y. Lee, J.-W. Hwang, S. Hong, C. Kim, T. G. Park, H. Lee, S. H. Hong, *Adv. Mater.* **2011**, *23*, 1971–1975; b) Q. Ye, F. Zhou, W. Liu, *Chem. Soc. Rev.* **2011**, *40*, 4244; c) M. J. Harrington, J. H. Waite, *J. Exp. Biol.* **2007**, *210*, 4307–4318; d) S. M. Kang, I. You, W. K. Cho, H. K. Shon, T. G. Lee, I. S. Choi, J. M. Karp, H. Lee, *Angew. Chem. Int. Ed.* **2010**, *49*, 9401–9404; e) H. O. Ham, Z. Liu, K. H. A. Lau, H. Lee, P. B. Messersmith, *Angew. Chem. Int. Ed.* **2011**, *50*, 732–736; f) S. M. Kang, S. Park, D. Kim, S. Y. Park, R. S. Ruoff, H. Lee, *Adv. Funct. Mater.* **2011**, *21*, 108–112; g) J.-H. Jeong, S. W. Hong, S. Hong, S. Yook, Y. Jung, J.-B. Park, C. D. Khue, B.-H. Im, J. Seo, H. Lee, et al., *Biomaterials* **2011**, *32*, 7961–7970; h) B. J. Endrizzi, G. Huang, P. F. Kiser, R. J. Stewart, *Langmuir* **2006**, *22*, 11305–11310.

[9] a) M. Vatankhah-Varnoosfaderani, A. GhavamiNejad, S. Hashmi, F. J. Stadler, *Chem. Commun.* **2013**, *49*, 4685–4687; b) Y. J. Oh, I. H. Cho, H. Lee, K.-J. Park, H. Lee, S. Y. Park, *Chem. Commun.* **2012**, *48*, 11895–11897; c) K. Kim, J. H. Ryu, D. Y. Lee, H. Lee, *Biomater. Sci.* **2013**, *1*, 783–790.

[10] K. Ni, X. Zhou, L. Zhao, H. Wang, Y. Ren, D. Wei, *PLoS ONE* **2012**, *7*, e41101.

[11] O. Zvarec, S. Purushotham, A. Masic, R. V. Ramanujan, A. Miserez, *Langmuir* **2013**, *29*, 10899.

[12] P. Sun, H. Lu, X. Yao, X. Tu, Z. Zheng, X. Wang, *J. Mat. Chem.* **2012**, *22*, 10035.

[13] D. G. Barrett, D. E. Fullenkamp, L. He, N. Holten-Andersen, K. Y. C. Lee and P. B. Messersmith, *Adv. Funct. Mater.*, 2013, **23**, 1111–1119.

[14] a) M. Vatankhah-Varnoosfaderani, S. Hashmi, A. GhavamiNejad, F. J. Stadler, *Polym. Chem.* **2013**, *5*, 512–523; b) K. Y. C. Lee, N. Holten-Anderson, J. H. Waite, *Methods of Making Self-Healing Polymer and Gel Compositions*, **2011**, WO2011084710 A1; c) M. S. Menyo, C. J. Hawker, J. H. Waite, *Soft Matter* **2013**, *9*, 10314–10323.

[15] a) N. Schweigert, A. J. B. Zehnder, R. I. L. Eggen, *Environ. Microbiol.* **2001**, *3*, 81–91; b) J. Monahan, J. J. Wilker, *Chem.Commun.* **2003**, 1672.

[16]. E. Mentasti and E. Pelizzetti, *J. Chem. Soc., Dalton Trans.*, **1973**, 2605–2608.

[17] a) G. N. L. Jameson, A. B. Kudryavtsev, and W. Linert, *J. Chem. Soc., Perkin Trans.*, 2001, 557–562; b) G. N. L. Jameson and W. Linert, *J. Chem. Soc., Perkin Trans.* 2, 2001, 563–568; c) G. N. L. Jameson and W. Linert, *J. Chem. Soc., Perkin Trans. 2*, 2001, 569–575.

[18] G. S. Longo, M. Olvera de la Cruz, and I. Szleifer, *Macromolecules*, **2011**, 44, 147–158.

[19] a) N. Holten-Andersen, M. J. Harrington, H. Birkedal, B. P. Lee, P. B. Messersmith, K. Y. C. Lee, and J. H. Waite, *Proc. Natl. Acad. Sci. USA*, **2011**, *108*, 2651–2655; b) B. J. Kim, D. X. Oh, S. Kim, J. H. Seo, D. S. Hwang, A. Masic, D. K. Han, and H. J. Cha, *Biomacromolecules* **2014**, *15*, 1579–1585; c) H. Zeng, D. S. Hwang, J. N. Israelachvili, and J. H. Waite, *Proc. Natl. Acad. Sci. USA*, **2010**, *107*, 12850–12853.

[20] R. H. Ewoldt and G. H. McKinley, *Rheology Bull.* **2007**, *76(1)***,** 4.

[21] C. Robertson and X. Wang, *Phys. Rev. Lett.* **2005**, 95.

[22] M. E. I. Badawy and E. I. Rabea, *Int. J. Carbohydr. Chem.* **2011**, *2011*, e460381.

[23] a) D. E. Fullenkamp, L. He, D. G. Barrett, W. R. Burghardt, P. B. Messersmith, *Macromolecules* **2013**, *46*, 1167–1174; b) D. G. Barrett, D. E. Fullenkamp, L. He, N. Holten-Andersen, K. Y. C. Lee, P. B. Messersmith, *Adv. Funct. Mater.* **2013**, *23*, 1111–1119; c) Z. Xu, *Sci. Rep.* **2013**, *3*, 2914.

[24] S.-M. Lee, E. Pippel, U. Gösele, C. Dresbach, Y. Qin, C. V. Chandran, T. Bräuniger, G. Hause, M. Knez, *Science* **2009**, *324*, 488–492.

[25] a) C. Persson, S. Berg, *J Mater Sci: Mater Med.* **2013**, *24*, 1–10; b) N. K. Guimard, K. K. Oehlenschlaeger, J. Zhou, S. Hilf, F. G. Schmidt, C. Barner-Kowollik, *Macromol. Chem. Phys.* **2012**, *213*, 131–143.

[26] a) Y. Ren, J. G. Rivera, L. He, H. Kulkarni, D.-K. Lee, P. B. Messersmith, *BMC Biotechnol.* **2011**, *11*, 63; b) L. M. Hight, J. J. Wilker, *J. Mater. Sci.* **2007**, *42*, 8934–8942; c) H. Xu, J. Nishida, W. Ma, H. Wu, M. Kobayashi, H. Otsuka, A. Takahara, *ACS Macro Lett.* **2012**, *1*, 457–460; d) E. Lallana, N. Tirelli, *Macromol. Chem. Phys.* **2013**, *214*, 143–158; e) H. Shao, G. M. Weerasekare, R. J. Stewart, *J. Biomed. Mater. Res. A*. **2011**, *97A*, 46–51.

Catechol rich polymers yield robust, self-healing hydrogels